

Macroporous Poly(vinyl alcohol) Foam Crosslinked with Epichlorohydrin for Microorganism Immobilization

Xue Bai,¹ Zhengfang Ye,² Yanfeng Li,¹ Yingxia Ma¹

¹State Key Laboratory of Applied Organic Chemistry, College of Chemistry and Chemical Engineering, Institute of Biochemical Engineering and Environmental Technology, Lanzhou University, Lanzhou 730000, China

²Department of Environmental Engineering, Key Laboratory of Water and Sediment Sciences of the Ministry of Education, Peking University, Beijing 100871, China

Received 20 June 2009; accepted 29 August 2009

DOI 10.1002/app.31420

Published online 27 April 2010 in Wiley InterScience (www.interscience.wiley.com).

ABSTRACT: Macroporous poly(vinyl alcohol) foam with epichlorohydrin as a crosslinking agent was investigated. The average molecular weight between crosslinks, crosslinking density, and mesh size were determined through the equilibrium swelling theory. The characterization of foams with different crosslinking ratios was also investigated through the testing of the thermal properties, specific surface areas, and diffusion coefficients. The biomass densities and activity yields were measured by detection of the protein concentration and oxygen uptake rate. Thermogravimetry and differential scanning calo-

rimetry tests showed an increase in the thermal stability and a decrease in the polymeric crystallinity with increasing crosslinking ratio. The biomass densities increased with increasing crosslinking ratio, with the highest value shown at 0.0638 ± 0.0093 g of volatile suspended solid (VSS)/g of carrier. However, the activity yields decreased with increasing crosslinking ratio, with the highest value at 69.38%. © 2010 Wiley Periodicals, Inc. *J Appl Polym Sci* 117: 2732–2739, 2010

Key words: crosslinking; macroporous polymers; networks

INTRODUCTION

Poly(vinyl alcohol) (PVA) is an ideal microorganism immobilization material because of its inherent good biocompatibility and desirable physical properties.¹ The entrapment of microorganisms in PVA carriers has turned out to be a successful method for the immobilization of such microorganisms.^{2,3} PVA carriers can also be infused with good mechanical properties and elasticity through the process of repeat freezing or chemical crosslinking. However, the entrapment of microorganisms in PVA carriers has some disadvantages, including microorganism activity loss during the freezing or crosslinking process, considerable limitations for the diffusion of large molecules, and susceptibility to degradation in media containing microorganisms. For practical applications, further research is thus needed to obtain new PVA carriers.

The adsorption of microorganisms on porous foams does not result in any toxicity that might lead to high microorganism activity.⁴ The addition of a pore-forming agent in the preparation process of a PVA carrier can result in high microporosity and macroporosity, which provide favorable conditions for the unhindered mass-transfer of substrates and

metabolites.⁵ Moreover, the large specific surface areas of porous PVA foams could greatly increase the adsorption ability. However, no reports on macroporous PVA foams as the carrier for immobilized microorganisms have been yet presented. Therefore, it is necessary to further investigate this efficient method of immobilization.

High stability and antibiodegradation properties can be achieved through chemical crosslinking. It is well known that PVA can be crosslinked because of its reaction with bifunctional or multifunctional compounds. Recently, several investigations have been reported on the thermodynamic, structural, and dynamic features of crosslinked PVA.^{6–8} However, the effects of crosslinking density on the biofeatures of PVA carriers have not yet been addressed.

In this study, macroporous PVA foams were crosslinked by epichlorohydrin to improve their stability. We investigated the characterization of the crosslinked macroporous foams with different crosslinking ratios by testing the swelling behavior, morphology, thermal properties, specific surface area, diffusion coefficient (*D*), and performance of the immobilized microorganisms.

EXPERIMENTAL

Materials

PVA, with a polymerization degree of 1750 and an alcoholysis degree higher than 99%, was purchased

Correspondence to: Y. Li (liyf@lzu.edu.cn).

from Lanzhou Vinylon Factory (Lanzhou, China). Epichlorohydrin, calcium carbonate, sodium hydroxide, hydrochloric acid, and other chemicals were all obtained from Beijing Chemical Reagent Factory (Beijing, China) and used without further purification.

Preparation of the crosslinked poly(vinyl alcohol) foam (CPVAF)

For the experiment, 100-mL hydrogel composites based on 15 g of PVA and 7.5 g of calcium carbonate were prepared and foamed by the addition of 5M stoichiometric hydrochloric acid. A freezing and thawing process was then used for molding to obtain the macroporous carrier.⁵ The molded foam was cut into approximately $2 \times 2 \times 2$ cm³ cubes and were then submerged into 200 mL of NaOH (1 M) containing different amounts of epichlorohydrin (EP) and stirred gently at 35°C for 2 h.

Characterization

Fourier transform infrared (FTIR) spectrometry (Thermo Nicolet, Nexus 670, Waltham, MA) was used to investigate the foam before and after crosslinking. Meanwhile, the morphology of the foam was examined using a scanning electron microscope (S-520 SEM, Hitachi, Japan). Thermogravimetric analysis (TGA; Netzsch, STA 499C, Germany) and a differential scanning calorimeter (PerkinElmer, Waltham, MA) were used to investigate the thermal behavior of the foams. The TGA thermogram was obtained during the heating step with temperatures ranging from 30 to 700°C at a rate of 10°C/min under a nitrogen purge (200 mL/min). The differential scanning calorimetry (DSC) thermogram (equilibrated with an indium standard, with each sample weighing 3–5 mg) was obtained with temperatures ranging from 50 to 250°C at a heating rate of 10°C/min under a nitrogen purge (60 mL/min).

The degree of swelling (S_w) was calculated as follows:

$$S_w = \frac{W - W_0}{W_0} \times 100\% \quad (1)$$

where W and W_0 denote the weights of the foam with absorbed water and the dry foams, respectively. The time duration for swelling was 24 h.

Crosslinked polymeric networks can be characterized conveniently by the crosslinking density (ρ), which is inversely related to the average molecular weight between crosslinks (M_c), according to the following equation:

$$\rho = \frac{1}{vM_c} \quad (2)$$

where v is the specific volume of the polymer (0.788 cm³/g).

Closely following Flory's derivation, we made a modification by taking into account that the crosslinkers were introduced between the polymer chains with a number-average molecular weight M_n . We calculated the crosslinking density when the crosslinkers were introduced between the polymer chains from the swelling data using eqs. (2) and (3):⁹

$$\frac{1}{M_c} = \frac{2}{M_n} - \frac{v}{V} \frac{\left[\ln(1 - v_{2,s}) + v_{2,s} + \chi(v_{2,s})^2 \right]}{v_{2,r} \left[\left(\frac{v_{2,s}}{v_{2,r}} \right)^{1/3} - \frac{1}{2} \left(\frac{v_{2,s}}{v_{2,r}} \right) \right]} \quad (3)$$

where M_n of PVA is known (72,000), v is the specific volume of PVA, V is the molar volume of the water (18.1 cm³/mol), and χ is the Flory polymer–solvent interaction parameter for PVA/water, which is 0.494. The true density of the dry foams, the volume fraction of the foam in the swollen foams ($v_{2,s}$), and the volume fraction of PVA in solution before crosslinking ($v_{2,r}$) were also calculated.¹⁰

The mesh size (ξ) defines the linear distance between consecutive crosslinks. It indicates the diffusional space available for solute transport and can be calculated as follows¹¹:

$$\xi = v_{2,s}^{-1/3} \left[C_n \left(\frac{2M_c}{M_r} \right) \right]^{1/2} l \quad (4)$$

where C_n is the Flory characteristic ratio (8.3), l is the carbon–carbon bond length (1.54 Å), and M_r is the molecular weight of the repeating unit of the polymer.

A modified method for measuring the specific surface area was used on the basis of the theory of the single-layer molecular absorption of methylene blue (MB) on a solid surface. The mass of adsorbed MB in the monolayer can be represented through the Langmuir equation¹²:

$$\frac{C_e}{q} = \frac{1}{q_{\max}} C_e + \frac{1}{bq_{\max}} \quad (5)$$

where C_e is the concentration of MB solution at the absorbing equilibrium (g/L), b is the adsorption constant (L/g), q is the mass of adsorbed MB in the monolayer (g of MB/g), and q_{\max} is the maximum mass of adsorbed MB in the monolayer (g of MB/g). The specific surface area was obtained by multiplication of q_{\max} by 2.45.¹³

D of the foams was calculated from the following relationship¹⁴:

$$F = 4 \left(\frac{D}{\pi t^2} \right)^{1/2} t^{1/2} \quad (6)$$

where F denotes the amount of penetrant (glucose) fraction at time t , D (cm²/s) is the apparent

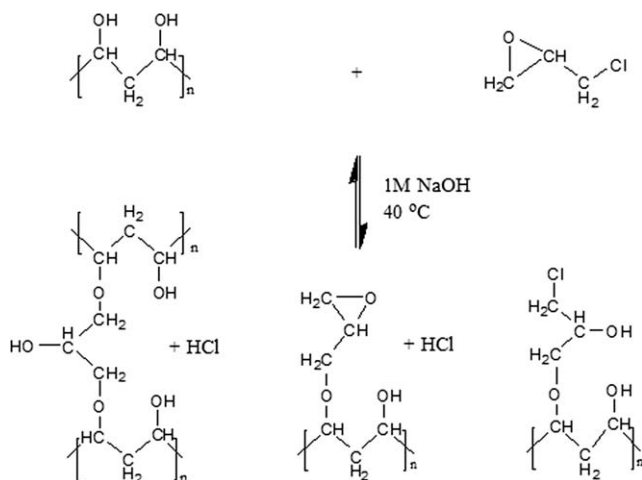


Figure 1 Equation of PVA crosslinking reaction with epichlorohydrin.

diffusion coefficient for the transport of the penetrant into the foams, t (s) is the time, and r is the radius of the cylindrical polymer sample. The glucose concentration was determined with the phenol sulfuric acid method.¹⁵

Microorganism immobilization experiments

Seed sludge was obtained from an aeration sludge tank of the Lanzhou (China) Petrochemical Sewage Treatment Plant. Concentrated activated sludge (10 g) was added to a 250-mL conical flask containing 100 g of sterilized wet macroporous PVA foam and 100 mL of medium consisting of 250 mg/L biochemical oxygen demand (BOD) and 25 mg/L NH_4^+-N .² The flask was then placed in an incubator and cultured for 7 days at a temperature of 30°C with sufficient aeration. The medium was then removed, after which the macroporous PVA foams containing the immobilized microorganisms were washed with saline. The biomass of the foams sample was estimated from the standard curve of volatile suspended solid (VSS) versus protein concentration.³ The cell protein of the foams was measured with the Coomassie brilliant blue method.¹⁶

RESULTS AND DISCUSSION

Crosslinking

The equation for the crosslinking reaction of PVA with EP is shown in Figure 1. In an ideal reaction, each EP molecule would react with two hydroxyl groups on the PVA chains; thus, each EP molecule could be expected to yield one hydroxyl group while consuming two hydroxyl groups of PVA. However, some side reactions, such as some EP molecules only reacting with one hydroxyl group and reacting with unreacted pendant epoxy or chloride groups, have been known to occur.

The FTIR spectrum of the uncrosslinked PVA foam and CPVAF are compared in Figure 2. The uncrosslinked PVA foam [Fig. 2(a)] showed a hydroxyl peak at 3422 cm^{-1} , whereas the hydroxyl peak of the CPVAF [Fig. 2(b)] was obviously weaker. This result indicated the occurrence of a crosslinking reaction. The stronger peak of CPVAF at 1100 cm^{-1} ($\nu_{\text{C-O-C}}$), compared with that of the uncrosslinked PVA foam, proved that the network structures were formed on the chains of the PVA foam with a certain amount of hydroxyl.

Meanwhile, PVA foams with different crosslinking ratios were prepared by the addition of different amounts of EP (according to the mass ratio of EP and PVA). The swelling degrees of the CPVAF carriers are shown in Table I. As shown, the swelling degree decreased with increasing amount of EP. This was attributed to the fact that the crosslinking reaction decreased the amount of hydroxyl groups (see Fig. 1), which was proportional to the foams' hydrophilicity. Therefore, the PVA foams manifesting the required degree of swelling could be prepared with different amounts of crosslinking agent.

The swelling data was used to evaluate the crosslinked structure of these foams. The molecular weight between crosslinks, the mesh size, and the crosslinking density were parameters used to characterize the porous structure of CPVAF (see Table I). The molecular weight between crosslinks and the mesh size of CPVAF were larger at lower crosslinking ratios. The mesh size of the hydrogels varied between 353.31 and 50.99 Å. The corresponding crosslinking density varied between 1.42×10^4 and $18.16 \times 10^4\text{ mol/cm}^3$.

A lower crosslinking ratio foam had longer strands between crosslinks or a looser network; it could swell more, as shown in the scanning electron microscopy (SEM) cross-sectional image (Fig. 3) of

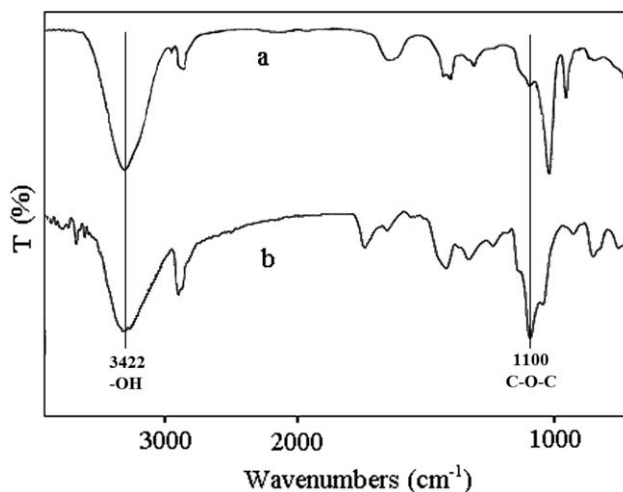


Figure 2 FTIR spectra of the (a) uncrosslinked PVA foam and (b) EP-CPVAF.

TABLE I
 M_c , ρ , and ζ of the PVA Foams at Various Crosslinking Ratios (X 's)

Carrier	X	S_w (%)	M_c (g/mol)	ρ (mol/cm ³ × 10 ⁴)	ζ (Å)
CPVAF-0	0	753.14 ± 23.75	8923 ± 596	1.42	353.31
CPVAF-1	1	521.76 ± 21.04	4674 ± 232	2.72	180.54
CPVAF-2	2	419.54 ± 24.78	1893 ± 563	6.70	95.13
CPVAF-5	5	375.75 ± 20.35	699 ± 254	18.16	50.99

the CPVAF taken after the swelling occurred. Figure 3 illustrates that typical microporous structures were present, with corresponding pore sizes that were larger at lower crosslinking ratios. As a result of the formation of crosslinked network structures, the physicochemical stability of the PVA foam increased, and the hydroxyl groups created a hydrophilic microenvironment for the metabolism of the immobilized microorganisms.

Carrier properties

Thermal analysis was performed to compare the differences in the polymeric arrangements of the samples. The thermogravimetry (TG) curves are presented in Figure 4. As shown, three transitions appeared in the thermogram of CPVAF-0 (the number after "CPVAF" indicates the crosslinking ratio). The first transition between 60 and 100°C referred to the loss of moisture that was present in the hydrophilic

material. The second stage, which occurred from 200 to 300°C, was regarded as the breakage of the grafted crosslinker, whereas the third step (occurring around 400°C) corresponded to the breakage of the main chain. The TG curves for CPVAF-1 also showed three main degradation steps. However, the weight losses of CPVAF-2 and CPVAF-5 were continuous and showed no marked difference in the degradation stages. In comparison with CPVAF-0, the weight loss of the first stage clearly decreased, which indicated a decrease in the foam hydrophilicity. These results corroborated the results of the swelling degree. Moreover, the degradation events occurred at higher temperatures; this denoted an increase in the foam thermal stability as a result of the crosslinking of the PVA foam by EP. This phenomenon was attributed to the gelation of the branched PVA, which had a broad range of composition.

The DSC curves are presented in Figure 5. The sample foams were included to establish a detailed

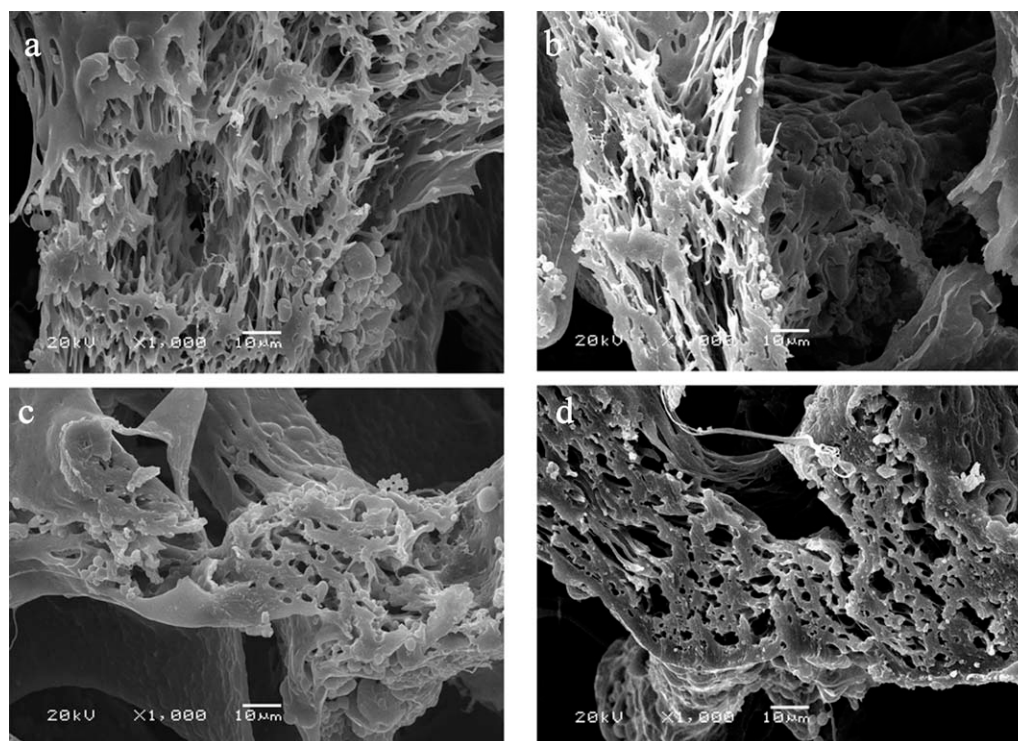


Figure 3 SEM cross-sectional image of the CPVAF frame: (a) CPVA-0, (b) CPVA-1, (c) CPVAF-2, and (d) CPVAF-5 at a magnification of 1000×.

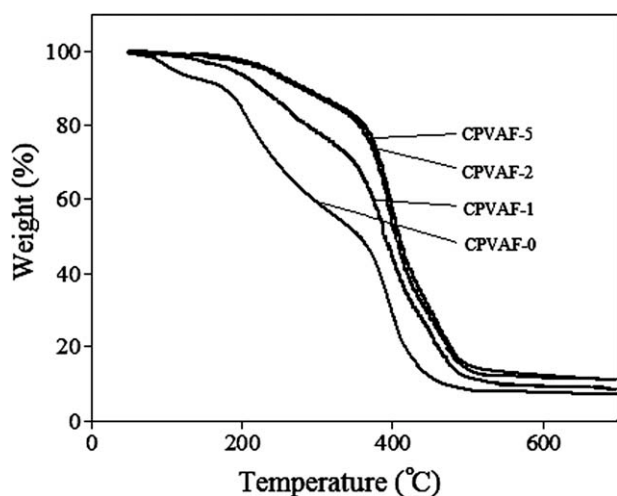


Figure 4 TG curves of the PVA foams at various crosslinking ratios.

behavior of the organization of polymeric chains. As shown in this figure, the CPVAF-0 carrier exhibited an endothermic peak at about 206.4°C, which corresponded to the melting temperature of PVA. The melting temperature of CPVAF increased along with increasing EP content. A rapid decrease in the enthalpy of fusion and melting temperature suggested that the crystallinity and perfection of the crystal structure decreased when the crosslinking ratio increased. This implied that the higher crosslinking ratio limited the mobility of the chains, which was quite reasonable.

Studies on the surface properties of the CPVAF carriers showed that all of the samples were characterized by high maximum uptake capacities (q_{\max} values) and specific surface areas. The q_{\max} values of MB of CPVAF-0, CPVAF-1, CPVAF-2, and CPVAF-5 were 66.23, 72.99, 77.34, and 81.97 mg of MB/g, respectively. The foams with a higher crosslinking

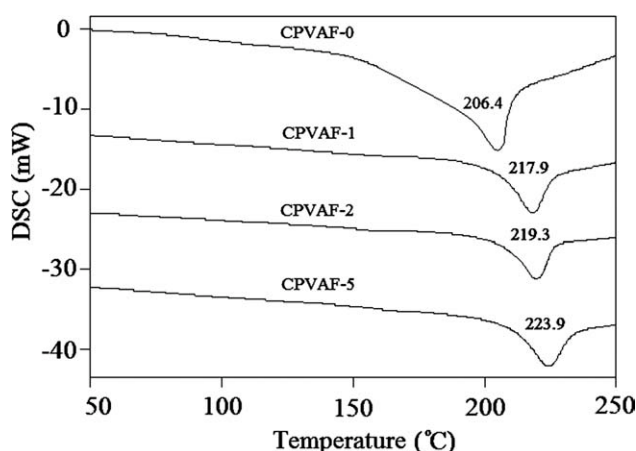


Figure 5 DSC curves of the PVA foams at various crosslinking ratios.

ratio had better MB adsorption capacity than those with a lower crosslinking ratio. As shown in Figure 6, the variation in the EP amount influenced the material properties and resulted in different values for the specific surface areas, which ranged from 162.25 to 200.82 m^2/g . The highest values for a specific surface area (200.82 m^2/g) were observed for the foam synthesized with the highest EP amount. This was attributed to the formation of crosslinked network structures when high EP concentrations were used.

Mass-transfer resistance between a bulk liquid and immobilized microorganisms is a limiting factor for the reaction of immobilized microorganisms in conventional carriers.¹⁷ The D values of the CPVAF carriers were between 8.34×10^{-3} and 9.48×10^{-3} cm^2/s (Fig. 6). The higher crosslinking ratio foam with the lower D attributed to it was more compact compared to a lower crosslinking ratio foam. This property seemed to limit the diffusivity of substrates with certain sizes, thereby increasing the energy required for diffusive transport through the CPVAF carrier. Moreover, the effective D s were universally higher in the CPVAF carriers than in any other type of PVA carriers prepared with different methods.^{17,18} The higher D of the CPVAF carrier may have arisen from the fact that CPVAF had many permeable pores that allowed substrate transport.

Microorganism immobilization

Scanning electron photomicrographs of the immobilized carriers are shown in Figure 7. It is clear that each carrier had comparatively regular pores and that the sizes of the pores of the four different carriers were strikingly different. High-crosslinking-ratio carriers had smaller pore sizes and a less

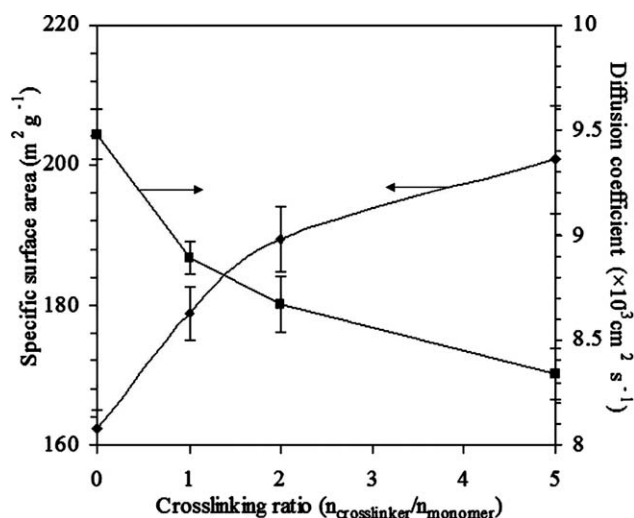


Figure 6 Specific surface areas and D values of the PVA foams at various crosslinking ratios; each data point is an average value taken from three samples.

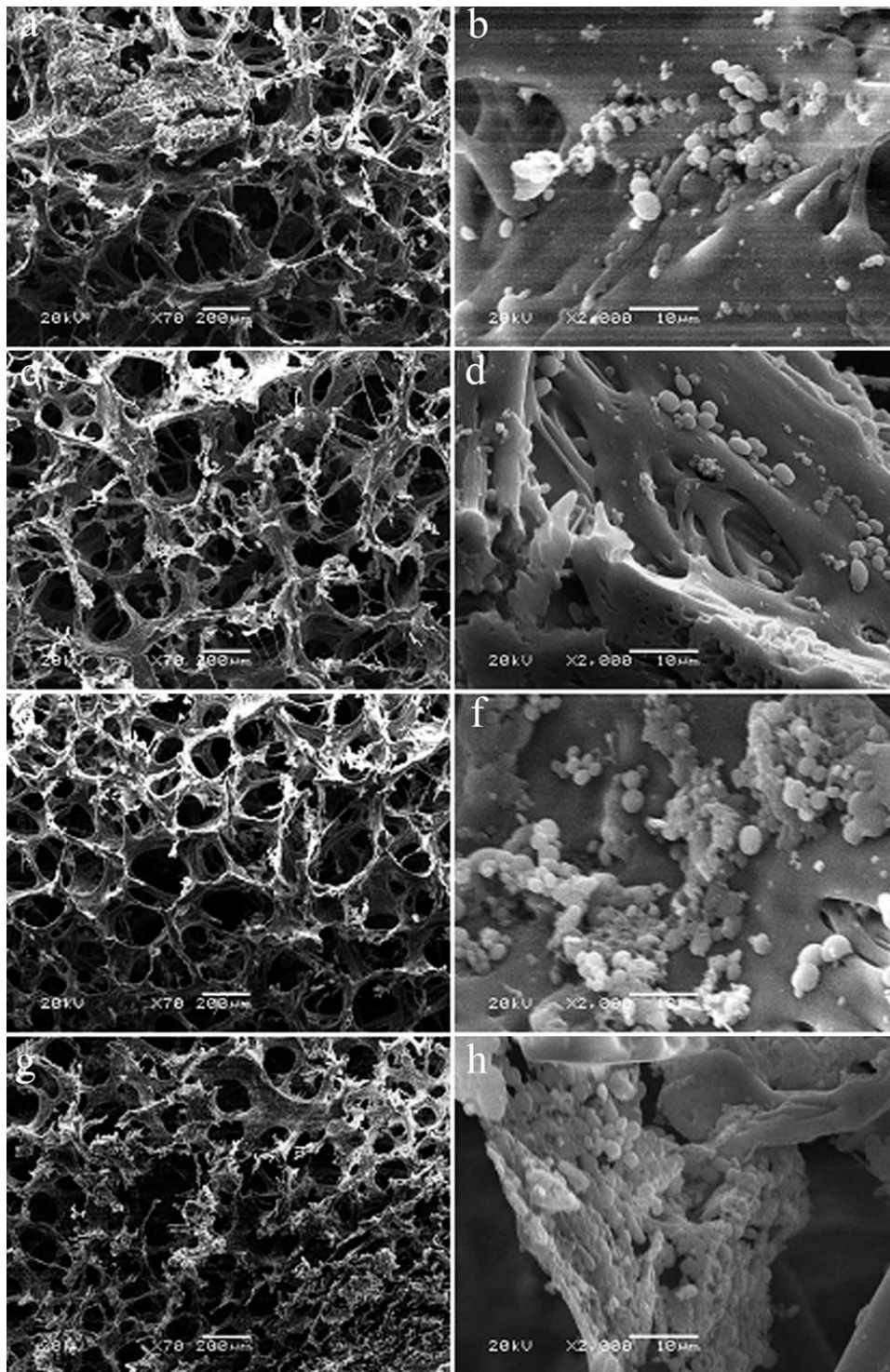


Figure 7 SEM photographs of the PVA foams at various crosslinking ratios in immobilized activated sludge. (a) CPVAF-0 at 70 \times , (b) CPVAF-0 at 2000 \times , (c) CPVAF-1 at 70 \times , (d) CPVAF-1 at 2000 \times , (e) CPVAF-2 at 70 \times , (f) CPVAF-2 at 2000 \times , (g) CPVAF-5 at 70 \times , and (h) CPVAF-5 at 2000 \times .

uniform porous structure than those with low crosslinking ratios. Because the total amount and ratio of pore-forming agents were uniform in the four carriers, these differences were attributed to the difference in the ratio of crosslinkers.

Microorganisms are extremely concentrated in high crosslinking ratio carriers but sparsely adhere to those with low crosslinking ratios (Fig. 7). The unreacted pendant had an obvious effect on the adsorption function of the CPVAF carriers, as the

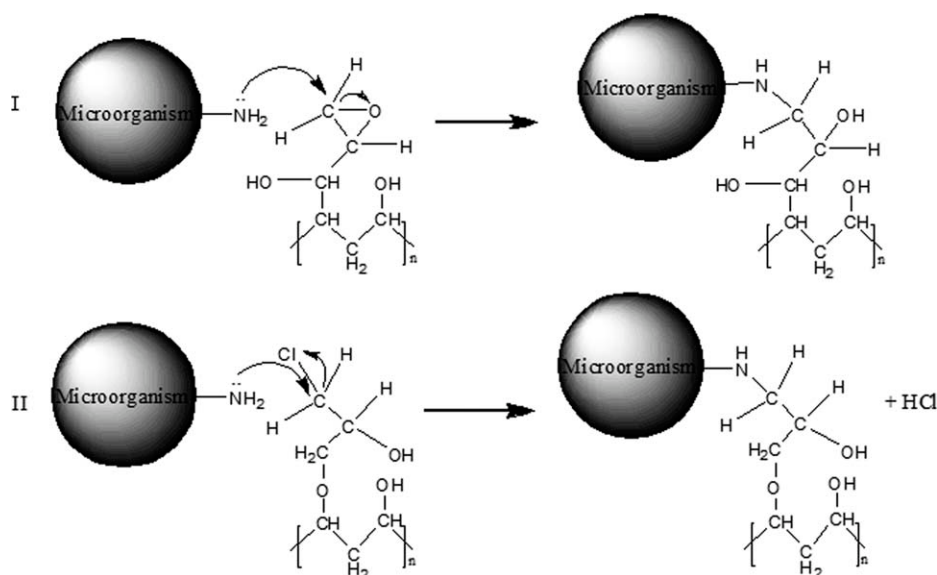


Figure 8 Immobilization of microorganisms onto the CPVAF carrier with pendant epoxy groups and chloride.

alkylation of the amino, phenolic, and thiol groups of the active microorganism proteins reacted with the pendant epoxy groups and chloride of the carriers.^{19,20} The opening of the oxide ring [Fig. 8(I)] and the leaving of chloride [Fig. 8(II)] in the reactions represent nucleophilic displacement on carbon. Therefore, the microorganisms adhered well to the high crosslinking ratio carriers, which thus increased the biomass density (Table II). Furthermore, high-crosslinking-ratio carriers had high specific surface areas, where microorganisms could attach and proliferate. This was particularly beneficial in culturing adhered microorganisms.

Although the use of higher crosslinking ratio carriers resulted in higher biomass densities (Table II), the activity yields were lower compared to those of the lower crosslinking ratio carriers. These values varied between 40 and 70%. The activity yield values of the CPVAF-0 and CPVAF-1 carriers were higher than those previously reported by Chen et al.³ for sludge immobilization in phosphorylated PVA gel beads. In that study, the activity yield was around 54%. The most probable reason for the relatively high activity yield was the macroporous CPVAF carrier, which had a specific oxygen mass transfer rate and is usually the bottle-neck step in an aerobic microorganism system.²¹ However, the respiratory activity (Table II) was lower in the CPVAF-2 and CPVAF-5 carriers; this indicated that high-crosslinking-ratio carriers could provide good habitats for microorganisms. This is because the respiratory activity of microorganisms was inhibited when the residual group of the cross-linked carriers reacted with the active proteins of the microorganism cells. With same reasoning, the activity yield of high-crosslinking-ratio carriers was relatively lower than those with low crosslinking ratios.

CONCLUSIONS

CPVAFs used as immobilization carriers were prepared at various crosslinking ratios to evaluate their properties. The degree of swelling and mesh size of the PVA foams decreased with increasing crosslinking ratio. In addition, TG and DSC tests showed an increase in the thermal stability and a decrease in the polymeric crystallinity with increasing crosslinking ratio. The specific surface area of the carriers increased with increasing crosslinking ratio, whereas *D* decreased because of a smaller mesh or pore size.

For the effects of pendant groups and high specific surface of the high crosslinking ratio carriers, the biomass density in the CPVAF carrier increased with increasing crosslinking ratio. Pendant epoxy groups and the chloride present in the carrier acted with groups of active microorganism proteins. As for the relatively low *D* value and toxicity of the high-crosslinking-ratio carrier, the activity yield was apparently lower than that of the low-crosslinking-ratio carriers.

TABLE II
Biomass Density and Activity of the PVA Foams at Various Crosslinking Ratios

Carrier	Biomass density (g of VSS/g of carrier)	Activity	
		Respiratory activity (O ₂ g of VSS/h)	Activity yield (%)
CPVAF-0	0.0429 ± 0.0105	11.76	69.38
CPVAF-1	0.0527 ± 0.0174	11.06	65.25
CPVAF-2	0.0626 ± 0.0081	8.08	47.67
CPVAF-5	0.0638 ± 0.0093	6.82	40.24

The CPVAFs possessed good properties for micro-organism immobilization. Their macroporous structure, swelling behavior, and functionalized groups make the foams potentially useful in the fields of biotechnology and biochemistry.

References

1. Lozinsky, V. I.; Zubov, A. L.; Titova, E. F. *Enzyme Microb Technol* 1997, 20, 182.
2. Zhang, L. S.; Wu, W. Z.; Wang, J. L. *J Environ Sci* 2007, 19, 1293.
3. Chen, K. C.; Lee, S. C.; Chin, S. C.; Houng, J. Y. *Enzyme Microb Technol* 1998, 23, 311.
4. Sakurai, A.; Nishida, Y.; Saito, H.; Sakakibara, M. *J Biosci Bioeng* 2000, 90, 526.
5. Li, Y.; Bai, X.; Men, X.; Yang, L. *Chin. Pat. CN 101348782A* (2008).
6. Figueiredo, K. C. S.; Alves, T. L. M.; Borges, C. P. *J Appl Polym Sci* 2009, 111, 3074.
7. Yang, X. M.; Zhu, Z. Y.; Liu, Q.; Chen, X. L. *J Appl Polym Sci* 2008, 109, 3825.
8. Wang, Y. L.; Yang, H.; Xu, Z. L. *J Appl Polym Sci* 2008, 107, 1423.
9. Bray, J. C.; Merrill, E. W. *J Appl Polym Sci* 1973, 17, 3779.
10. Kawai, T. *J Polym Sci* 1958, 32, 425.
11. Hickey, A. S.; Peppas, N. A. *J Membr Sci* 1995, 107, 229.
12. Yu, Y.; Zhuang, Y. Y.; Wang, Z. H. *J Colloid Interface Sci* 2001, 242, 288.
13. Hang, P. T. *Clays Clay Miner* 1970, 18, 203.
14. Saraydin, D.; Oztop, H. N.; Karadag, E.; Oztop, A. Y.; Isikver, Y.; Guven, O. *Process Biochem* 2002, 37, PII S0032.
15. Masuko, T.; Minami, A.; Iwasaki, N.; Majima, T.; Nishimura, S. I.; Lee, Y. C. *Anal Biochem* 2005, 339, 69.
16. Bradford, M. M. *Anal Biochem* 1976, 72, 248.
17. Yeom, C. K.; Lee, K. H. *J Appl Polym Sci* 1996, 59, 1271.
18. Adoor, S. G.; Prathab, B.; Manjeshwar, L. S.; Aminabhavi, T. A. *Polymer* 2007, 48, 5417.
19. Atia, K. S.; El-Batal, A. *J Chem Technol Biotechnol* 2005, 80, 805.
20. Santos, J. C.; Paula, A. V.; Nunes, G. F. M.; de Castro, H. F. *J Mol Catal B* 2008, 52–53, 49.
21. Yu, J. A.; Ji, M.; Yue, P. L. *J Chem Technol Biotechnol* 1999, 74, 619.